Design of a Magnetic Dual-Needle Biopsy Capsule Robot Resilient to Cross-Infection and Mixed Contamination

Bo Ye, Zuolei Chen, Shufang Wang, Sixian Liu, Bo Wang, Zhi Shu, Yihan Xu, Baoshun Liu, Shoujun Dai, Anh Nguyen, *Member, IEEE*, Amit Krishna Dwivedi, *Member, IEEE*, and Sheng Liu, *Fellow, IEEE*

***Abstract*—Capsule robots have demonstrated great potential for comfortable, non-invasive diagnosis of the gastrointestinal tract. With the advancement of research in capsule endoscopy, its functionality has expanded from initial imaging capabilities to include biopsy operations. However, most biopsy capsule robots cannot separately place the tissues obtained during biopsy. The cross-infection caused while using the same biopsy tools at different biopsy sites, and inaccurate results due to mixed contamination of the pathological tissues, still need to be addressed. This paper presents a novel magnetic Dual-needle Biopsy Capsule Robot (DBCR) design to solve this problem. The capsule design was simplified into a double needle switching and anchoring structure in the capsule, modelled based on a retractable pen's extension and retraction control mechanism. Additionally, the design was equipped with magnets and springs of different sizes to complete the needle switching mechanism and extract the tissue samples. The force of the external control magnet on the magnet inside the capsule was simulated to determine the control distance to achieve different functions and ensure sampling reliability. The prototype was designed, manufactured, and tested using in vitro experiments. The achieved results show that the proposed design of the DBCR is promising and can potentially obtain biopsy samples, preventing cross-infection and mixed contamination.*Note to Practitioners*— The proposed DBCR design can potentially address the limitations of current systems in obtaining biopsy samples, mainly by preventing cross-infection and mixed contamination, in double-needle designs. The proposed design offers a dual-needle storage and switching mechanism based on a retractable pen-inspired linear-to-rotational motion conversion system for compartmentalized sampling and the gradient magnetic field control of embedded magnets and springs to ensure needle activation only during biopsy. Thus, the proposed design finds its suitability for use in biopsy.**

Received 23 October 2025; revised 28 December 2025; accepted 25 February 2026. Date of publication 8 April 2026; date of current version 5 May 2026. This article was recommended for publication by Associate Editor L. Zhang and Editor F. Ficuciello upon evaluation of the reviewers' comments. *(Corresponding authors: Amit Krishna Dwivedi; Sheng Liu.)*

Bo Ye, Zuolei Chen, Shufang Wang, Sixian Liu, Bo Wang, Zhi Shu, and Shoujun Dai are with the School of Artificial Intelligence, Hubei University, Wuhan 430062, China (e-mail: yebo@hubu.edu.cn; 202421121013012@stu.hubu.edu.cn; 202221116012852@stu.hubu.edu.cn; 1349456413@qq.com; BoBo@stu.hubu.edu.cn; shuzhi@stu.hubu.edu.cn; 15212681094@163.com).

Yihan Xu and Baoshun Liu are with Manchester Metropolitan Joint Institute, Hubei University, Wuhan 430062, China (e-mail: 2643496599@qq.com; lbs2786962992@qq.com).

Anh Nguyen is with the Department of Computer Science, University of Liverpool, L69 3BX Liverpool, U.K. (e-mail: anh.nguyen@liverpool.ac.uk).

Amit Krishna Dwivedi is with the School of Engineering, University of Warwick, CV4 7AL Coventry, U.K. (e-mail: Amit.Dwivedi@warwick.ac.uk).

Sheng Liu is with the School of Integrated Circuits, Wuhan University, Wuhan 430072, China (e-mail: shengliu@whu.edu.cn).

Digital Object Identifier 10.1109/TMRB.2026.3680996

***Index Terms*—Biopsy, capsule robot, dual needle capsule, force sensors, wireless capsule endoscope.**

I. Introduction

THE risk of gastrointestinal diseases in humans is alarming. According to the statistics of the World Health Organization, more than 10 million people die of gastrointestinal diseases each year worldwide [1]. The emergence of small bowel diseases is growing rapidly [2]. Most small bowel cancers are accidentally discovered, during surgery for inflammatory bowel disease, or sometimes at an advanced stage due to the poor prognosis [3], [4]. Therefore, early diagnosis of small bowel diseases can effectively reduce mortality due to small bowel cancer. In recent years, the emergence of capsule endoscopy has greatly relieved the discomfort caused during endoscopy [5]. For this reason, wireless capsule endoscopy has become an important technology for the diagnosis of small bowel diseases [6]. The initial dependence of capsule endoscopes is solely on gastrointestinal motility, which not only takes a long time but also causes the omission of lesions. To solve this issue, an actively controllable model was proposed [7], [8], [9]. By adding coils, magnets, and micro brakes, the posture and position of the model can be adjusted, and a more thorough examination of the small intestine can be achieved [7], [8], [9]. For instance, Song et al. [10] developed an adaptive magnetic levitation-based control system for capsule robots, achieving 3- Degrees of Freedom (DOF) suspended translation and attitude adjustment through coordinated electromagnetic coils. This approach overcomes the limitations of traditional magnetically driven capsules in terms of insufficient DOF and poor environmental adaptability, though limited to locomotion. Similarly, Chen et al. [11] proposed a data-driven control method employing dynamic input constraints and nonlinear resistance compensation to mitigate motion disturbances and model uncertainties in complex gastrointestinal environments. It should be noted that, although the aforementioned magnetic control technologies made significant progress in terms of motion degrees of freedom and environmental adaptability, their functionality remains largely confined to the optical imaging of lesions. However, image diagnosis is not a complete diagnosis, and hence, a biopsy is required for some lesions. This could be achieved using wireless biopsy capsule endoscopy. The relevant background literature listing the functions of the capsules, achieved

TABLE I
SUMMARY OF THE PREVIOUS WORKS

References	Function of the capsule	Experimental results	Remarks
[7]	Small intestine imaging	It has an auxiliary effect on the treatment of small intestine diseases.	Short power supply time by intestinal peristaltic movement
[8]	Small intestine imaging	It has been used in clinic and achieved promising results.	Imaging only. Good for passive motion.
[9]	Lesion location detection	The larger the lesion, the higher the success rate. The success rate for 3 cm polyps was 81%.	The observation accuracy of small lesions was not promising.
[10]	Motion control	The maximum controllable inclination Angle is 45°.	Potential mechanical delay issues
[11]	Motion control	Inhibition of motor disturbances in complex gastrointestinal environments	Dynamic changes of intestinal nonlinear resistance
[12]	Fine needle biopsy	Control the linear extension of the biopsy needle to collect tissue with a volume of up to 5 mm^3.	The cost of the equipment is high.
[13]	biopsy forceps	The maximum extension length of the biopsy is 3 mm, enabling the effective collection of tissue.	The mechanical transmission of the mechanism has a significant response delay, and the samples are subject to potential mixed contamination.
[14]	biopsy forceps	Effectively perform a biopsy and avoid accidental injuries.	It has a high design complexity and is prone to environmental interference in practical applications.

results and limitations of the models are summarized in Table I.

Several designs of biopsy capsule robots were suggested in the literature. For instance, Le et al. [12] proposed a biopsy capsule endoscope driven by an external electromagnetic field. Through the coupling effect between the external electromagnetic field and the built-in ring permanent magnet, this capsule can achieve four-degree-of-freedom active movement. Moreover, it uses a rotating magnetic field to drive the screw transmission mechanism, controlling the linear extension of the biopsy needle to collect tissues (with a volume of up to 5 mm^3). Its advantage lies in the real-time visualization of the biopsy process and the fact that it does not consume the energy of the internal battery, which significantly improves operation safety. However, this solution relies on a complex external electromagnetic system, resulting in high equipment costs.

In another article, Guo et al. [13] designed a magnetically driven biopsy capsule robot based on a cam structure. This robot uses a three-axis Helmholtz coil to generate a rotating magnetic field, which drives the built-in radially magnetized permanent magnet to drive the propeller for propulsion. It also uses the cam mechanism to synchronously control the expansion and contraction of three groups of miniature barbed biopsy forceps. Its innovation lies in the symmetrical barb design, which can reduce tissue damage, and the 3D printed resin shell that takes into account both corrosion resistance and lightweight. The experiments showed that the robot can move stably in a liquid environment, and the maximum extension length of the biopsy is 3 mm. However, the mechanical transmission response of the mechanism has a significant delay, and the fluid resistance during high-speed movement leads to a decrease in propulsion efficiency, which limits its application in complex intestinal environments. In another study, Khameneh et al. [14] developed a capsule robot integrated with a fail-safe mechanism. It adopted an axial and radial dual-permanent magnet design, controlling the pose of the robot through an external uniform magnetic field, and used the principle of the magnetic spring to achieve the triggering and automatic retraction of the biopsy forceps. The advantage of this solution is that the biopsy tool is automatically locked when the power is off, avoiding accidental damage. However, the optimization of the distance and angle between the magnets depended on finite element analysis, resulting in a high design complexity. In addition, precise control of the opening and closing angle of the biopsy forceps required a highly uniform magnetic field, which is vulnerable to environmental interference in practical applications. Therefore, although all the above-mentioned devices could collect sample tissues, the models still have issues such as high equipment costs, high design complexity, the limitation of only having a single biopsy structure for biopsy, and the mixed storage of tissue samples [7], [8], [9], [10], [11], [12], [13], [14].

To address the persistent challenges of sample cross-contamination and structural complexity in existing biopsy capsule robots, this study introduces a novel dual-needle biopsy strategy inspired by the mechanism of retractable pens. Retractable pens employ an internal spring-based mechanism that converts linear actuation into rotational motion, enabling reliable extension and retraction of the tip. Drawing upon this principle, we developed a magnetically controlled Dual-needle Biopsy Capsule Robot (DBCR). By modulating the distance between an external magnet and the capsule [17], the system drives internal magnetic components to transform linear displacement into rotational movement, thereby facilitating precise switching between two independent biopsy needles. This design enables separate tissue acquisition from two distinct lesions, effectively eliminating cross-contamination and mixed sample issues, and significantly enhancing the reliability of pathological diagnosis [18]. Furthermore, needle biopsy induces smaller mucosal wounds compared to blade-based excision, promoting improved post-procedural recovery. The same biomimetic mechanism is also utilized for achieving luminal anchoring of the capsule via controlled extension and retraction of the tip [19]. The dual-needle design can store two tissues separately in different syringes, and the gradient magnetic field controls the internal magnet to achieve the switching and extension of the needle, to achieve the extraction of tissues from two lesions [15], [16]. A device similar to a retractable

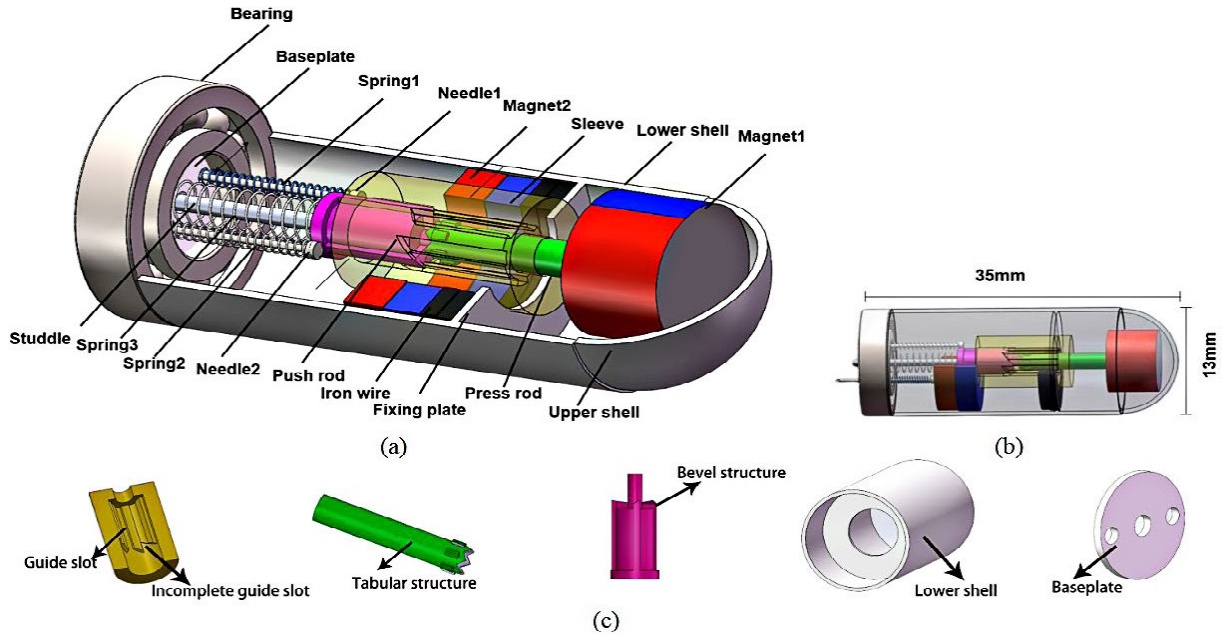

Fig. 1. (a) Structure of the two-needle biopsy capsule robot. (b) Specific dimensions of the proposed DBCR. (c) From left to right are the Sleeve section, Press rod, Push rod, Lower shell and Baseplate.

pen structure is embedded in the proposed DBCR, which can convert linear motion into rotational motion to achieve the switching of the needle. Three embedded permanent magnets (a large magnet to control the switching of the needle and two small magnets to control the output of the needle), Spring1, Spring2 and Magnet2 were used to control the extension of the needle, avoiding the problem that the needle will trigger incorrectly when it does not need to be extended. The dual-needle design can effectively avoid the mixed contamination of two different kinds of lesion tissues, and the sampling of two different tissues is more convincing for the detection of one lesion. A prototype of the double-needle biopsy capsule was developed using 3D printing, and its performance was tested using in-vitro biopsy experiments.

The rest of the paper is organized as follows. Section II presents the material and methods used in the proposed design. Section III presents a discussion on the prototype and production of the capsule. The simulation and experimental results are presented in Section IV, and the discussion is reported in Section V. Finally, concluding remarks are made in Section VI.

II. Materials and Methods

A. Design of the Proposed Model

The design of the proposed DBCR is shown in Fig. 1(a). The designed capsule was 35mm long and 13mm in diameter (as shown in Fig. 1(b)). The capsule consists of a biopsy part, a permanent magnet, and a needle switching part. Spring 1 and Spring 2 (wire diameter: 0.2 mm, outer diameter: 2.8 mm, full copper) are integrated into the biopsy mechanism, while Spring 3 (wire diameter: 0.3 mm, outer diameter: 3 mm) serves as the core elastic element in the needle switching assembly. Among these, the needle switching part comprises a press rod, Magnet1 fixed on the press rod, a push rod, and a sleeve. The sleeve assembly—composed of a baseplate, Spring 3, a staddle, and a bearing—is fixed on the lower shell. In this design, the sleeve mechanism plays a crucial role in guiding, constraining, and locking the push rod during the switching process. Its internal structure is inspired by the retractable pen mechanism, which converts linear motion into rotational motion through the interaction between bevels and spiral guide slots. This configuration enables the push rod to rotate precisely while maintaining alignment within the confined capsule space. Moreover, the sleeve mechanism provides a self-locking function: once the external magnetic field is removed, Spring 3 pushes the push rod upward, and the bevel structure re-engages with the incomplete guide slot on the sleeve, preventing unintentional needle extension. Such a design not only ensures smooth needle switching under magnetic control but also enhances mechanical reliability and resistance to accidental triggering during operation. The downward movement of Magnet1, controlled by the external magnet, enables the push rod to disengage from the guide slot of the sleeve (Fig. 1(c)),

When the external magnetic field disappears, the push rod is subjected to the restoring force of the spring. Due to the contact between the bevelled serrations of the push rod and the press rod, a torque is generated, thereby converting linear motion into the rotational motion of the push rod. The push rod and the baseplate are connected through Spring 3, while the baseplate is fixed on the bearing. The rotation of the push rod drives the baseplate to rotate, allowing different pins to switch to the side where Spring 2 is located. One end of the studdle is fixed on the push rod, and the other end passes through the hole in the baseplate. When the bevel structure of the push rod becomes stuck in the incomplete guide slot of the sleeve during its downward movement (as shown in Fig. 1(c)), the studdle extends but achieves anchoring [20].

We adopted a dual-needle configuration rather than using more needles because the actuation range of Magnet2 is limited to 0–180°, which precisely accommodates two needles.

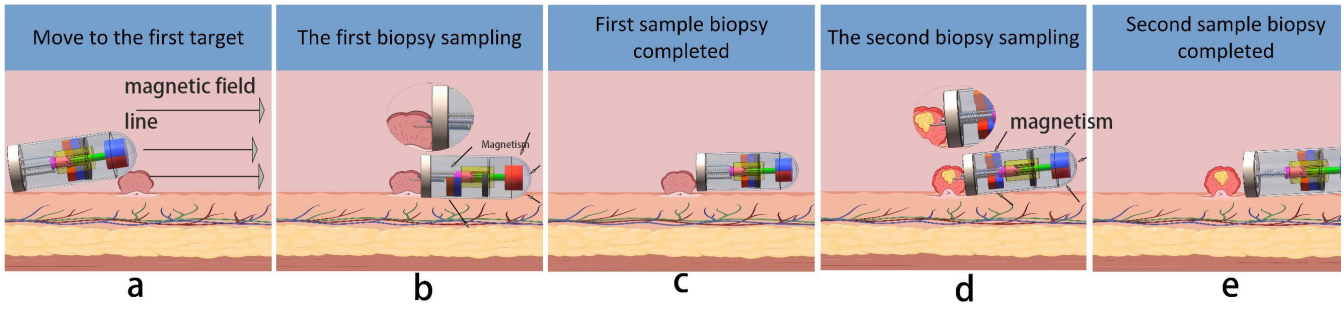

Fig. 2. Schematic diagram illustrating the biopsy procedure using the proposed capsule robot. Figs. (b) and (d) presents a magnified view of the procedure. The first and second needles protrude as illustrated in Figs. (d) and (e). The smaller pictures on Figs. (b) and Figs (d) are partial pictures of the needle insertion into the tissue.

Incorporating additional needles could result in simultaneous extensions of multiple needles, potentially causing unintended tissue injury. To achieve independent and accurate magnetic control, a square axial magnet and a cylindrical radial magnet were employed as the external permanent magnets.

B. Biopsy Procedure

A schematic diagram of the biopsy procedure performed using a BCR is shown in Fig. 2. The capsule first enters the intestine from oral swallowing, and then the needle extension, needle switching, and capsule movement of the capsule robot are controlled by varying the different distances between the external magnet (cylindrical or square external magnet) and the robot capsule in the intestine [21]. In order to ensure the extension and retraction of the experimental needle, the side of the iron wire was made to coincide with the Fixing plate surface, and the iron wire was fixed on the Fixing plate surface. Magnet2 was attracted to the iron wire due to the magnetic force. The holes on both sides of the Baseplate were located where the needle sticks out. On the inner wall of the Baseplate fixed Bearing, one end of Spring1 and Spring2 was fixed on the Baseplate, the center of the spring was opposite to the center of the hole, and the other end was fixed together with the needle. The internal magnet can be used as a driving magnet to control the movement of the capsule. The internal magnets, Magnet1 and Magnet2, are controlled by the magnetic field gradient and are subject to the magnetic control of the external magnet. By precisely controlling the distance of the external magnet from the capsule, DBCR can align itself along with the required target, control the downward movement of Magnet2, drive the needle to extend, and implement the sampling, so that the collection of diseased tissue in the first place is completed. The Magnet1 can be used as a control to retract the anchor. Then, an external magnet drives the BCR to move, the needle retracts from the tissue into the hole, reaches the second lesion, and anchors out to complete the biopsy of the second lesion. The external drive capsule endoscope is mainly driven by an electromagnetic coil or an external permanent magnet. As the control of the electromagnetic coil is complicated and the operating area is relatively small, we adopt an external permanent magnet to drive the capsule robot. The biopsy procedure shown in Fig. 2 using the proposed robot capsule is briefly discussed here. This paper is mainly devoted to the study of biopsy, without adding cameras. The experimental

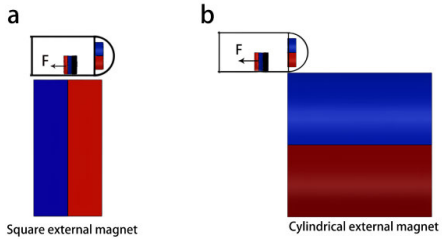

Fig. 3. (a) The position of the square external magnet relative to the DBCR when the needle is extended. (b) The position of the cylindrical external magnet relative to the DBCR when the needle switching is implemented. Please note, the N pole of the magnet is shown in blue, and the s pole is shown in red.

study is based on a sample, and the location of the pathological tissue is determined artificially in advance.

In Fig. 2(a), the position and posture of the capsule are adjusted using the external magnet acting on all internal magnets in the capsule so that the capsule is close to the first lesion [22]. At this time, the magnets in the capsule can be used as driving magnets for capsule movement. The distance of the external magnet is controlled, the capsule is driven to move, and the needle is switched and extended without the accidental protrusion of the needle.

The first biopsy sampling procedure using the proposed robot capsule is shown in Fig. 2(b). When the external magnet is near, the capsule position can be adjusted to determine the direction due to the magnetic force. During the sampling process, the position of the cylindrical external magnet is kept close to the top of the capsule as shown in Fig. 3(a), and the magnetic force is applied to Magnet1 to push the bevel structure of the rod into the Incomplete guide slot (illustrated in Fig. 1(c)) in the Sleeve so that the Studdle extends out, that is, the anchor extends out. At the same time, due to the extension of the anchor, the Baseplate rotates 60° and drives the needle to rotate 60° so that the position of the square external magnet is close to the middle of the capsule as shown in Fig. 3(b). This extends the needle to get the tissue from the first lesion. As the spring force is less than the force of insertion into the tissue, the needle is trapped in the tissue (Fig. 2(b)).

In Fig. 2(c), once the first sample biopsy is completed, the cylindrical external magnet pulls Magnet1 down (as shown in Fig. 3(b)), causing the Bevel structure on the Push rod to slide into the Guide slot of the Sleeve, retracting the Studdle which

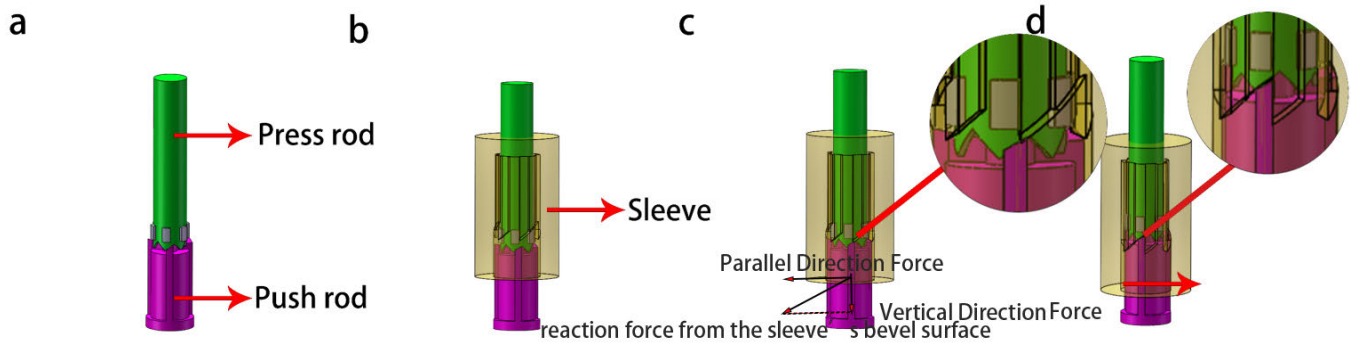

Fig. 4. Schematic to illustrate the switching process of the needle.

is also known as the anchored retracting. At the same time, the push rod rotates 60° and drives the Needle on the Baseplate to rotate 60°. The square external magnet acts on the capsule and drives the capsule to move forward. At this time, the first needle protrudes from the tissue due to the forward movement of the capsule and then retracts into the capsule shell due to the elasticity of the spring on the needle.

When the second lesion is reached, the above process is repeated. The cylindrical external magnet drives the magnet downward, making the Studdle protrude. At the same time, the top rod is rotated 60°. The square external permanent magnet drives Magnet2 downward, making the second biopsy needle protrude and obtain the tissue from the second lesion (as shown in Fig. 2(d)). Finally, the square permanent magnet drives the capsule to move forward, making the biopsy needle protrude from the tissue and retract into the capsule shell due to the action of the spring. Thus, the biopsy procedure of the two lesions is accomplished (Fig. 2(e)).

C. Switching Mechanism Analysis

The switching mechanism primarily involves the structural components responsible for extending and retracting the pen nib in a stylus. The process of converting the linear motion during downward pressing into rotational motion involves the conversion of torque [23]. In this context, the external magnet driving Magnet1's downward motion can be considered as the force applied to the Press rod. During the act of pressing the Press rod, the forces acting on it can be decomposed into two components: one perpendicular to the Press rod's direction, and the other parallel to it. The force in the perpendicular direction will result in the linear motion of the Press rod, pushing the Push rod, while the force in the parallel direction will generate a torque, causing the Push rod to rotate. The analysis of these forces in both directions is as follows:

1) **Vertical Direction (Linear Motion):** The force in the vertical direction will be equal to the product of the mass of the Press rod and Magnet1, multiplied by the acceleration. In the absence of friction, it can be expressed as:

$$F = ma. \tag{1}$$

Where F is the force in the vertical direction, m is the combined mass of the Press rod and Magnet1, and a is the linear acceleration.

2) **Parallel Direction (Rotational Motion):** The force in the parallel direction will generate a torque, causing the Push rod to rotate around an axis. The magnitude of the torque is equal to the product of the parallel force applied to the Press rod and the lever arm. The lever arm is the distance from the point of force application to the axis of rotation. The torque can be expressed as:

$$\tau = r \times F. \tag{2}$$

where τ is the torque, F is the parallel force applied to the Press rod, and r is the lever arm distance from the point of force application to the axis of rotation.

When the external magnet no longer acts on Magnet1, the Push rod will move upward due to the action of Spring3, and the Bevel structure of the Push rod will get stuck in the Incomplete guide slot, at which time the anchor will extend out, so the switch will be accompanied by the extension of the anchor. The force required for Studdle to penetrate tissue can be calculated by considering the material's elastic modulus and the geometric shape of the needle. In this case, this force can be expressed as:

$$F = EA. \tag{3}$$

where E represents the equivalent elastic modulus of the tissue, A is the cross-sectional area of the needle. Based on [24], Young's modulus of the small intestine mucosa is approximately in the range of 0.1 to 1 kilopascal (kPa) [25]. The Press rod's lateral surface features six protrusions and indentations, which guide it during its insertion and retraction, with a serrated edge at the bottom. The Push rod has only three Bevel structures. The needle switching mechanism enables the conversion of linear motion into rotational motion, and the Push rod is the only part that rotates, while the Press rod and Sleeve remain stationary. Guide slots are located on the Sleeve (as shown in Fig. 1(c)). The Bevel structures in the Push rod slide up and down on these Guide slots. The switching process is illustrated in Fig. 4 [26].

When the Press rod makes contact with the Push rod (Fig. 4(a)), initially pressing down on the Press rod exerts downward pressure on the Push rod, causing it to move downward. At this point, the Push rod and Press rod are in linear contact (Fig. 4(b)). As the Press rod pushes the Push rod out of the Guide slot (Fig. 4(c)), with no restrictions from the Guide slot, the Bevel structure on the Push rod disengages from it. The Bevel structure on the Push rod then makes linear contact with the Incomplete guide slot on the Sleeve's inclined surface. A spring at the bottom provides an upward force to the Push rod, causing it to slide to the right and enter the Incomplete guide slot (Fig. 4(d)). In this case, the Bevel structure of the Push rod is the incomplete Guide slot stuck in

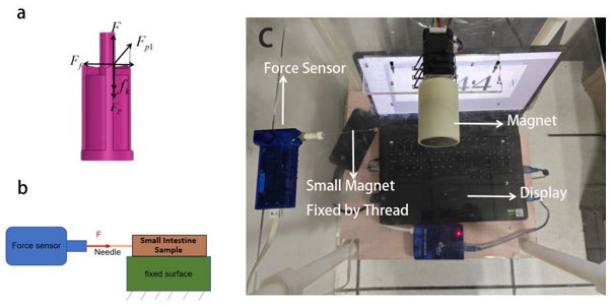

Fig. 5. (a) Schematic diagram of the experimental setup for measuring the force required for the biopsy needle to obtain tissue. F is the spring force, FP is the force of the Press rod to the Push rod, fk is the downward friction force in contact with the sleeve, F_{P1} is the force of spring3 against the Push rod upward to make the Push rod inclined surface, Ff is the parallel direction of the Push rod inclined friction component (b) Test bench sketch of force required to measure biopsy needle to obtain tissue. (c) Photograph of the experimental setup used to measure the biopsy needle sampling force.

the Sleeve. Compared with the sliding of the Bevel structure into the Guide slot, the Push rod is closer to the lower part of the capsule at this time. This causes the Studdle attached to the Push rod to extend downward, that is, anchoring. Fig. 5(a) illustrates the forces acting on the Bevel structure at this moment. When the Bevel structure of the Push rod slides into the Guide slot or the Incomplete guide slot, the force analysis of the contact surface between the Bevel structure and the Incomplete guide slot is carried out.

$$F_f < F_{p1} cos\theta \tag{4}$$

$$F < f + F_{p.} \tag{5}$$

Then, we repeat the above steps. The Bevel structure on the Push rod slides into the Guide slot, which results in the retraction of anchoring. When the Bevel structure on the Push rod enters the Incomplete guide slot, it rotates by 60°. This process is repeated, rotating by another 60°, for the second biopsy. To perform a third biopsy and complete the needle switching, the process is repeated three times or more, resulting in a total rotation of 180°, completing the needle switch.

D. Force Analysis for Tissue Acquisition/Sampling

To effectively obtain tissue samples, in this work, a 19 Gauge subcutaneous injection needle was selected as the biopsy tool [15]. The needle has an outer diameter of approximately 1.10mm and an inner diameter of around 0.55mm. The needle features an angled bevel with a serrated edge [27], [28]. To determine the force required for the biopsy needle to penetrate the tissue, given the unique structure of the biopsy needle for which there is no specific formula, we set up an experimental apparatus as shown in Fig. 5(b). The biopsy needle was secured at one end of a Force sensor (Manufacture: DISLab, Model: LW-6001), and the needle was inserted into a specimen to obtain the required biopsy samples. The force required to obtain tissue samples was measured, and this experiment was repeated 10 times, resulting in an average force of 0.44N [29], [30], [31].

III. Prototype Development

To validate the feasibility of the proposed DBCR model, we designed and manufactured a prototype, as shown in Fig. 6. It has a diameter of 13mm and a length of 35mm. Considering the control of the diameter and length of the DBCR, Magnet1 was chosen as a cylindrical radial magnet with an outer diameter of 10mm, a thickness of 5mm, and an N35 magnet (remnant magnetization of 1.18T). To avoid excessive magnetic interference, a cylindrical iron wire with a diameter of 2mm and a length of 6mm was selected and bent to match the curvature of the cylindrical shell precisely. The wire is made so that when the external permanent magnet is removed, the Magnet2 returns to its original position because of the suction force with the wire. The Magnet2 was a radial magnet with a diameter of 3mm. To ensure an adequate tissue sample and smooth tissue extraction without excessive tearing, a commonly used 19G injection needle was chosen, with two serrated hooks carved on the sloped part of the Needle. The Upper shell, Lower shell, Baseplate, and Sleeve were manufactured using 3D printing technology [32]. Due to limitations in 3D printing precision and materials, it was unable to achieve the required accuracy for the details of the Press rod and Push rod. Therefore, we used commercially available Press rod and Push rod structures commonly found in styluses. Spring3 is a fully copper spring with a wire diameter of 0.2mm, an outer diameter of 3mm, and a height of 20mm. Spring1 and Spring2 are fully copper springs with a wire diameter of 0.2mm, an outer diameter of 2.8mm, and a height of 10mm.

The tolerances of the push-rod and sleeve components were controlled within ±0.05 mm using high-resolution 3D printing and post-machining. This precision was found to be sufficient to ensure repeatable motion of the needle actuation mechanism under magnetic control.

IV. Simulation and Experimental Results

A. Test of Needle Extension Performance

The mechanical formula only provides a theoretical description under ideal conditions. To test whether the forces between the magnets can meet the requirements for needle extension and retraction performance, as well as the precise control distance of the external magnet for different BCR functions [33], we used finite element analysis software (Maxwell) to simulate the magnitude of the magnetic force acting on the magnets inside the capsule. The simulation screenshots of the magnetic force of the square external magnet and the cylindrical external magnet are shown in Fig. 7. As the external magnetic force on Magnet2 must be greater than the force between the Iron wire and Magnet2 to ensure that Magnet2 slides downward under the influence of the external magnet, the simulation indicates that the maximum force between the Iron wire and Magnet2 is approximately 1.05N. To ensure that the force is greater than 1.05N, the external magnet was positioned within 4mm of Magnet2. Therefore, we measured the change in the force experienced by Magnet2 at distances of 1mm, 2mm, 3mm, and 4mm from the capsule (Fig. 8(a)). Based on the dimensions of the DBCR, the distance that Magnet2 moves downward inside the capsule is 10mm. When

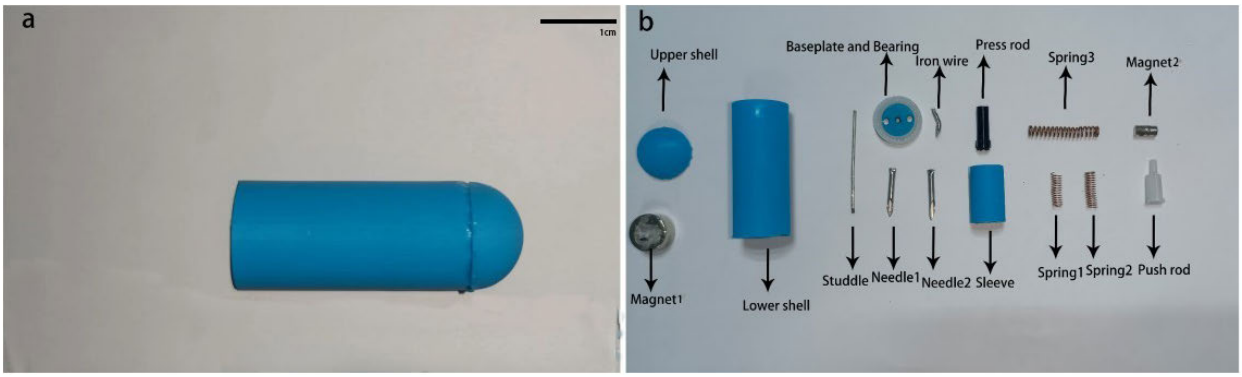

Fig. 6. (a) Image of the developed biopsy capsule prototype. (b) Various components of the capsule.

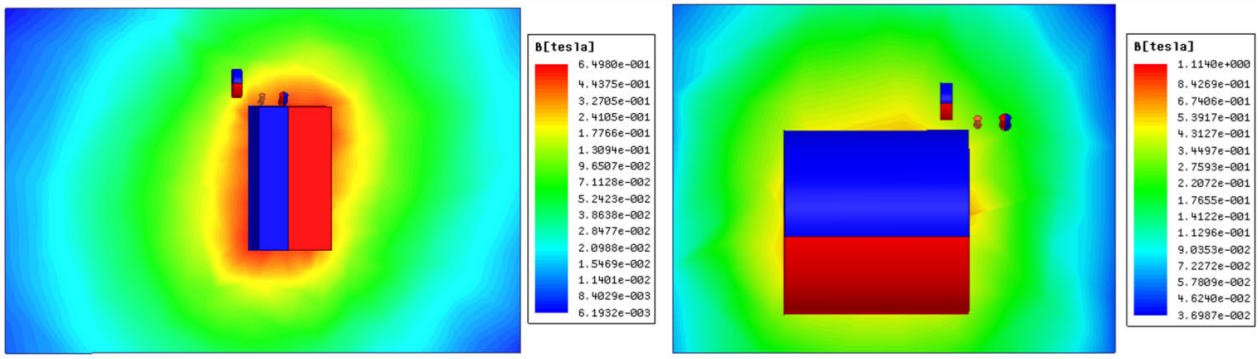

Fig. 7. Simulation screenshot of magnetic flux density in the space around the square external magnet and cylindrical external magnet. It also indicates the relative position of the external magnet and the internal magnet during simulation.

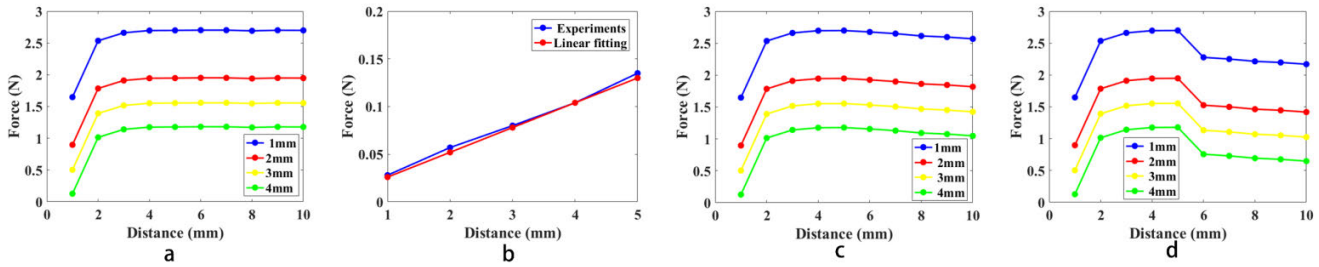

Fig. 8. (a) Force of the square external Magnet on Magnet2. (b) The force acting on Spring1. (c) The force acting on Magnet2 minus the force acting on Spring1. (d) Subtract the force of Spring1 from the force of Magnet2 and subtract the force of acquiring tissue.

it moves down 5mm, it encounters the spring, and the spring force is shown in Fig. 8(b). Magnet2's force due to the external magnet minus the spring force is illustrated in Fig. 8(c). Additionally, the needle starts to extend at the 5mm position, requiring a force of 0.4N to overcome tissue penetration, as shown in Fig. 8(d). At this point, all forces are greater than 0. Therefore, it can be concluded that the external magnet can extend the needle when it is positioned within 4mm of the capsule.

B. Test of Needle Retraction Performance and Capsule Movement Performance

When the needle penetrates the tissue, the small elasticity of the spring means that only the square external magnet can drive the entire capsule to move, allowing the needle to exit the tissue and retract into the capsule shell [34]. In order to better distinguish the magnetic field gradient, we simulated the changes in the force due to the varying distance of the external magnet relative to the capsule. The key to the simulation is that the square external magnet controls the biopsy needle to penetrate the tissue, then the external permanent magnet is removed, and the spring cannot retract on its own. This indicates that the spring's force is less than the force required for tissue penetration. As shown in Fig. 8(b), the force required for skin penetration is 0.4N, while the maximum force exerted by the spring is 0.13N, indicating that it cannot retract on its own. Treating the capsule as a whole, we determined the change in force as a function of the distance between the external magnet and the capsule (Fig. 9). In order to prevent the Studdle from accidentally sticking out, that is, interfering with Magnet1, we made Magnet1 move downward. It can be seen that the maximum stretched length of Spring3 during the protruding process of Studdle is 3.5mm, and the maximum stretched length of spring when Studdle springs back is also 3mm. The corresponding spring force is 0.42N, and the force of Studdle inserting into the tissue is 0.55N. Therefore, the force of the external magnet on Magnet1 is less than 0.97N, as shown in Fig. 9. That is, the distance between the

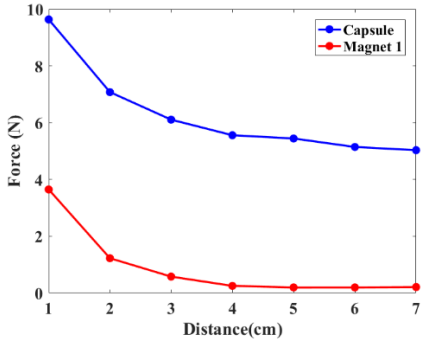

Fig. 9. Force on the DBCR and force on Magnet1 as the distance between the square external magnet and the DBCR changes.

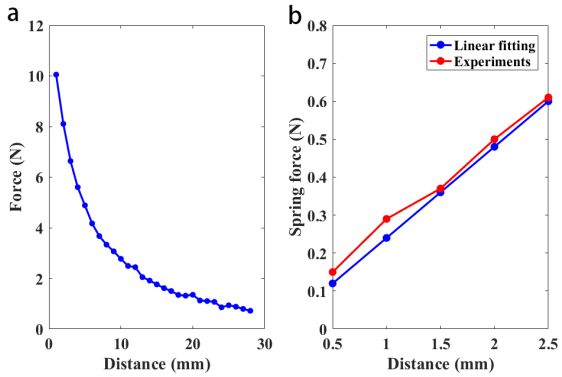

Fig. 10. (a) The force of cylindrical external Magnet on Magnet1 (b) Spring3 force analysis.

external magnet and the capsule should be greater than 20mm. The farther the external magnet is from the capsule, the less magnetic force it exerts on Magnet1. Therefore, the external magnet should be at a distance greater than 20mm from the capsule when controlling its movement. At the same time, the weight of the capsule is 0.053N, and the force required for the needle to penetrate the tissue is 0.4N. Hence, the external magnet's force on the DBCR should be greater than 0.453N to drive the capsule's movement with minimal friction against the intestinal wall [35]. Fig. 9 shows that the external magnet's force on the entire capsule is significantly greater than its force on the entire capsule is significantly greater than its force on Magnet1. Therefore, when the external magnet drives the DBCR's movement, we only need to consider the interference of the external magnet's force on Magnet1. According to the simulation, when the external magnet drives the capsule's movement, the distance between the external magnet and the capsule should be greater than 20mm.

C. Needle Switching Force Size Test

During the needle-switching process, two situations need to be considered. To better differentiate the magnetic field gradient, we replaced the magnets with cylindrical radial magnets with a diameter and length of 50mm and an N38 magnet (remnant magnetization of 1.23T). In the first situation, when the Studdle is extended, meaning it is anchored out, during the anchoring extension process, Spring3 undergoes a maximum deformation of 3.5mm. Similarly, during the anchoring retraction, the spring undergoes a maximum deformation of 3mm, corresponding to a force of 0.42N. The force required for anchoring into the tissue is 0.55N. Therefore, the force exerted by the external magnet on Magnet1 must be greater than 0.97N to ensure successful anchoring. This is shown in Fig. 10(a), which represents the force exerted by the external magnet on Magnet1 during the process. The spring force should gradually increase in Fig. 10(b). Thus, it can be concluded that the external magnet can complete needle switching within 25mm from the internal magnet for both the anchoring extension and anchoring retraction scenarios. In the second situation, when anchoring retracts, the spring's maximum deformation remains at 3.5mm, and it needs to overcome the force of 0.55N required for penetration. The results achieved were in line with the first scenario. In the second situation, when anchoring

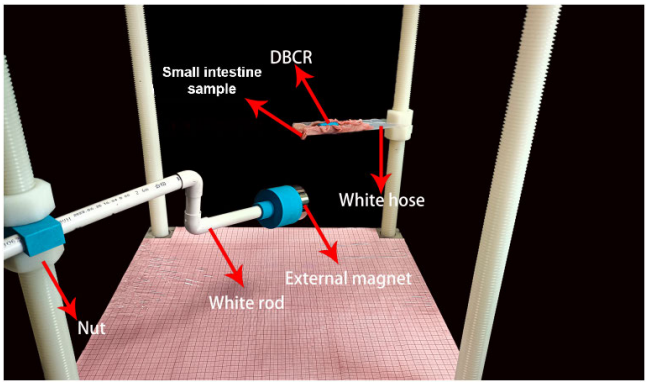

Fig. 11. In vitro biopsy experimental set-up used in this work.

retracts, the spring's maximum deformation remains at 3.5mm, and it needs to overcome the force of 0.55N required for penetration. The results achieved were in line with the first scenario. Additionally, as the cylindrical external magnet has some magnetic interference with Magnet2, the magnetic force generated by the external magnet between Magnet2 is less than 1.05 N. Through simulation, it can be determined that the maximum force will not exceed 1.05 N. Taking all these factors into consideration, the distance between the cylindrical external magnet and the capsule should be less than 25mm.

D. In-Vitro Experiments of Dual-Needle Biopsy Capsule Robot

Based on the experiment discussed in the previous section, it was established that precise control of the external magnet's position relative to the capsule is necessary for the design to perform the various functions of the capsule. To validate the capsule's motion and sampling during the biopsy process, we set up the experimental set-up as shown in Fig. 11. It allows us to control the external magnet's forward and backward movement as well as its rotation around the small intestine using the white rod passing through the slider. The distance between the magnet and the small intestine can be controlled by the nut at the slider.

To better observe the capsule's status during the biopsy process, we fixed it with a white hose (Fig. 11). We installed the required external permanent magnets at the end of the support. Under the drive of the magnets, the DBCR moved within the small intestine for biopsy. Fig. 12 shows the motion

TABLE II
COMPARISON OF DIFFERENT TYPES OF CAPSULES

Capsule type	Biopsy Tool	Biopsy Method	Biopsy Depth	Biopsy Tissue Volume	Anchoring	Size/ Dimension	Type of Drive
Biopsy Robot 1 [34]	tt-grippers	One-time inspection	epidermis	200-300 mm^3	inexistence	31.5×30mm	Magnetic actuation
ALICE [35]	blade	One-time inspection	epidermis	5 mm^3	inexistence	12×32mm	electromagnetic actuation
Biopsy robot 3 [36]	blade	One-time inspection	epidermis		exist	40×15mm	gastrointestinal motility
MTS [37]	blade	Multiple tests at once	epidermis	5 mm^3	inexistence	9×24mm	Magnetic actuation
MABC [38]	needle	Multiple tests at once	5mm	0.35 mm^3	inexistence	15×32mm	Magnetic actuation
DBCR (this work)	Double needle	Double needle and double test	5mm	2.4 mm^3	exist	13×35mm	Magnetic actuation

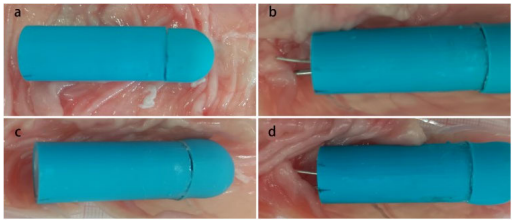

Fig. 12. The process of the 4th Ex Vivo Biopsy. (a) Failure to reach the first lesion. (b) Biopsy of the first lesion. (c) Failure to reach the second lesion. (d) Biopsy of the second lesion.

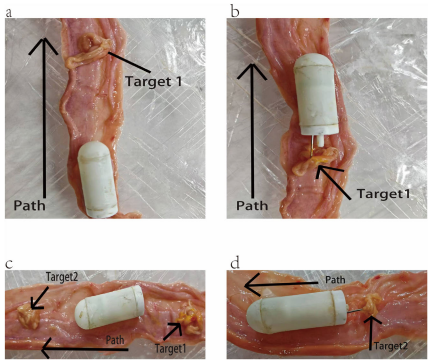

Fig. 13. The process of in vitro fluorescence testing. (a) Capsule positioning before biopsy at Target 1. (b) Biopsy performed at Target 1. (c) Capsule repositioning toward Target 2. (d) Biopsy performed at Target 2.

of the DBCR under the influence of the external magnet. Fig. 12(a) depicts the process of reaching the target location, Fig. 12(b) represents reaching the first target for biopsy, where both needles are deployed simultaneously to provide anchoring stability. One needle serves as an anchoring point to fix the capsule body, while the other performs the tissue acquisition. This configuration prevents undesired capsule displacement and ensures accurate force transmission during sampling. The completion of the first biopsy is shown in Fig. 12(c) and reaching the second lesion location, where the second needle is used for biopsy, is shown in Fig. 12(d). Since the shape of the biopsy samples is irregular, we performed the biopsy process ten times and estimated the volume of the obtained samples. The average volume was 2.4 mm^3.

E. Ex Vivo Fluorescence Leakage Test

To evaluate potential cross-contamination between the two biopsy channels, an ex vivo fluorescent leakage experiment was conducted using fresh porcine small intestine sample. The intestinal lumen was irrigated with saline to maintain a physiologically relevant moist environment. As illustrated in Fig. 13(b), a high-concentration sodium fluorescein solution was injected during the biopsy of Target 1 using Needle 1. Following needle retraction and successful switching to Needle 2, the capsule was navigated to Target 2. The subsequent biopsy of Target 2 was performed with Needle 2, as shown in Fig. 13(d). The capsule was then disassembled for fluorescent imaging examination of the second needle's chamber and outlet. This experiment was repeated five times under identical conditions. The fluorescence intensity within the second needle chamber was quantified using ImageJ software and compared against that of the first needle chamber (positive control) and a pristine Needle 2 chamber (negative control, no biopsy procedure).

V. DISCUSSION

A. Results Comparison

In order to highlight the performance of the proposed DBCR design, we selected five biopsy robot performance indicators to compare the proposed work with recent articles available in the literature. The comparison results are reported in Table II. Comparison of the tissue sample quantities obtained under different experimental conditions are illustrated in Fig. 14. Measuring the sample quantity reflects the biopsy efficiency of the capsule and verifies whether sufficient tissue can be collected for pathological analysis. The target sample quantity for an effective biopsy is typically 3–5 mg. The proposed DBCR achieves an average sample quantity within this range, demonstrating reliable sampling capability. The tissues biopsied were particularly small [36], and the recovery rate of biopsy tools was 7%. where recovery rate is defined as the ratio of collected tissue mass to the target biopsy mass, indicating the sampling efficiency of the biopsy mechanism. The capsule design in [37] aimed to obtain the diseased tissue for biopsy using a blade. Blade incision can only obtain the surface of the lesion for biopsy, and the diseased tissue within the lesion epidermis for biopsy [37]. The biopsy capsule reported in [36] is larger and driven by gastrointestinal peristalsis, so the process will be relatively slow [38]. Furthermore, the capsule robots in [39] and [40] are simple, the biopsy tissue is relatively large, and the needle can also be biopsied below the epidermis, the tissue biopsied can only be mixed together, and the blade and the fine needle are repeatedly biopsied at different lesions, which is easy to cause cross infection and the accuracy of biopsy tissue detection is decreased. Compared

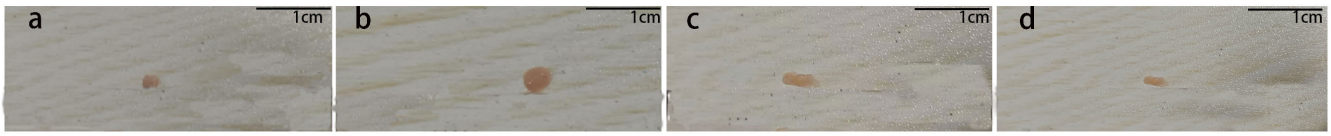

Fig. 14. (a) Tissue sample obtained from the 4th Needle1 biopsy. (b) Tissue sample obtained from the 4th Needle2 biopsy. (c) Tissue sample obtained from the 5th Needle1 biopsy. (d) Tissue sample obtained from the 5th Needle2 biopsy.

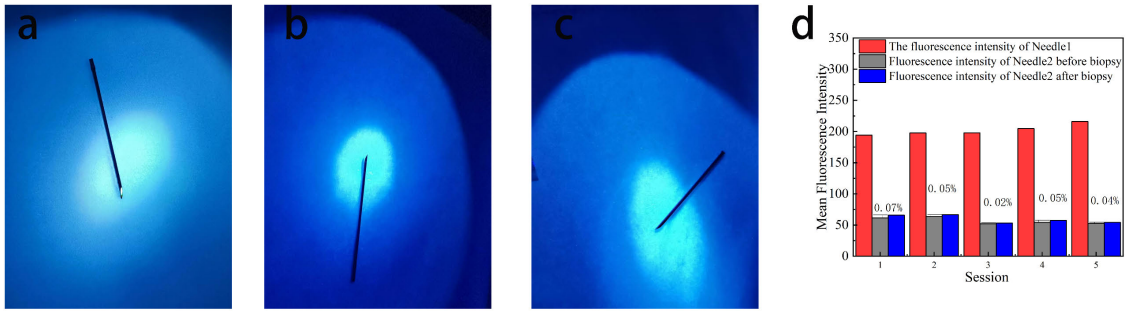

Fig. 15. Ex vivo fluorescence leakage assessment under UV illumination following the first complete biopsy cycle. (a) Ultraviolet (UV) illumination of Needle 1 after injection of sodium fluorescein solution. (b) UV illumination of Needle 2 without biopsy. (c) UV illumination of Needle 2 following the biopsy procedure. (d) Quantitative analysis of the average fluorescence intensity and the improvement rate from five independent experiments.

to the capsule robots discussed above, the capsule design proposed in this work can be used as a double-needle double-examination capsule, and thus two different lesions can be biopsied with two biopsy tools, and the tissues from the two lesions can be placed in different pinholes for preservation. This "distributed storage" design allows more efficient utilization of the capsule's internal space by avoiding the use of a single large cavity that would otherwise result in wasted volume. Moreover, the compact switching mechanism occupies less space than a single large storage chamber, enabling the dual-needle configuration to achieve greater effective storage capacity.

In traditional endoscopic biopsies [41], [42], when multiple diseased tissues are encountered, the doctor will take multiple samples one by one, placing each sample in a different container. The goal is to ensure that each sample can be correctly identified and that subsequent pathological analysis can accurately determine where each sample came from [43] and [44]. In the double-needle biopsy in this study, first of all, the double-needle design makes the storage space larger and obtains enough tissues for biopsy. Secondly, tissues with different lesions can be stored separately, avoiding cross-infection between tissues and improving the accuracy of biopsy by imitating the process of successive collection by the traditional endoscope. Additionally, an ex vivo fluorescence leakage experiment confirmed the feasibility of the distributed storage structure. Its capability to resist both cross-contamination and sample mixing was evidenced by the comparison of pre- and post-biopsy fluorescence intensity, as presented in Fig. 15(d).

B. Limitations and Future Work

While the DBCR can effectively perform biopsies, there are still significant challenges in terms of the robot's anchoring mechanism. The solid needles used for anchoring are positioned near the bottom diameter of the capsule robot, making it less reliable for insertion into tissue in cases of smaller tumours or areas with mild small intestine folds, where anchoring is required. However, with closed-loop control, synchronized positioning, and increased control over various degrees of freedom, it is possible to align the capsule's anchoring mechanism with the location of the lesion [45]. In the future, we will devote ourselves to the positioning and joining of the research group to form a complete closed-loop control system. Additionally, this study validates the feasibility of an endoscopic camera within the dual-needle biopsy capsule, providing the potential for real-time visualization of the biopsy process. Different magnetic field sources or larger permanent magnets could be employed to adapt the platform for patients of varying body sizes. Furthermore, adding a second camera to observe the biopsy process would enhance the reliability of tissue acquisition during biopsies [47]. A limitation of the current prototype is that short-duration needle contact is used to assist positional stabilization during biopsy, which may introduce potential mucosal injury risks under unexpected disturbances. Future work will focus on safer stabilization strategies, such as compliant or flexible anchoring structures and geometry-optimized designs, to further reduce tissue stress and improve clinical safety. In addition, a single-point anchoring mechanism may provide limited resistance to rotational torque on compliant and lubricated gastrointestinal mucosa, potentially resulting in pivoting behavior. In addition, anchoring validation performed in a rigid tube may overestimate stability compared to real biological tissue. These limitations highlight the need for future evaluation on ex vivo or in vivo tissue and the exploration of enhanced anchoring strategies. Meanwhile, regarding actuation safety, the significant separation between the biopsy actuation distance (<4 mm) and the capsule locomotion distance (>20 mm) provides a substantial spatial safety margin exceeding 16 mm. This margin considerably exceeds the typical displacement ranges induced by patient motion or respiration [46]. Moreover, needle deployment requires a sustained magnetic force sufficient to overcome both the spring resistance and the attractive force between Magnet 2 and the

iron ring, thereby preventing unintended needle release due to transient disturbances or minor positional inaccuracies. Biopsy is designed to be performed only after the capsule is successfully anchored and properly aligned, which further mitigates the risk of accidental actuation in clinical settings. Future investigations will include extreme-condition and error-safe motion testing to systematically evaluate the potential for inadvertent biopsy triggering under fault scenarios. From a clinical perspective, the current prototype measures 13 mm $\times$35 mm, exceeding the dimensions of standard capsule endoscopes (approximately 11 mm $\times$26 mm). This increase in size may elevate the risk of capsule retention, particularly at anatomical narrowings such as the pylorus. However, this risk is not universal and is highly dependent on patient-specific anatomy, the presence of gastrointestinal strictures, and the intended deployment region of the capsule. Importantly, the proposed DBCR is not intended to replace routine whole-gastrointestinal capsule endoscopy, but rather to serve as a platform for targeted biopsy in specific clinical scenarios. At the current stage, capsule retention risk may be mitigated through clinically established strategies, such as pre-procedural patency capsule screening or restriction of deployment to anatomically suitable regions. From an engineering perspective, further miniaturization and systematic in vivo evaluation will be essential in future work to reduce retention risk and enhance clinical applicability. Miniaturization of the DBCR is feasible through optimization of magnet geometry and magnetization, replacement of 3D-printed components with thinner integrated structures, and the adoption of advanced manufacturing processes such as injection molding or micro-machining. It should be noted that the 4 mm actuation distance represents an idealized near-field condition used for feasibility analysis rather than a clinically realistic scenario. In practical applications, deeper actuation would require stronger magnetic sources or alternative magnetic field generation strategies. The force analysis presented in this work is intentionally simplified and should be interpreted as a first-order engineering estimate rather than a predictive biomechanical model. Although some capsule components were fabricated via 3D printing for rapid prototyping, the core load-bearing and motion-transmission elements of the linear-to-rotational bistable mechanism—namely the push rod, plunger, and sleeve—were directly adapted from a commercially available retractable ballpoint pen mechanism with mature and repeatable tribological characteristics. Consequently, detailed modeling of frictional contact, surface tribology, and fracture-dominated needle–tissue interaction was beyond the scope of this study. Incorporating experimentally informed friction parameters and fracture mechanics-based tissue models will be an important focus of future work as the system advances toward higher-fidelity validation.

VI. Conclusion

In this work, we propose a DBCR and a prototype measuring 38 mm $\times$13 mm has been manufactured. By controlling external magnets acting on various internal magnets, needle switching and needle extension can be achieved. This allows for a single endoscopic biopsy in the capsule to extract tissue from two different lesions, ensuring the reliability of lesion verification and reducing contamination between tissue specimens. Experimental results demonstrate that the DBCR can effectively obtain the samples from two different lesion sites, successfully completing the biopsy procedure and thus can help in tacking the cross-infection and mixed contamination during the biopsy. To directly evaluate cross-contamination prevention, a quantitative ex vivo dye-based leakage experiment was conducted in this study. Fluorescein sodium solution was introduced through one biopsy needle, followed by needle retraction, switching, and activation of the second needle. Both qualitative ultraviolet fluorescence imaging and ImageJ-based quantitative analysis confirmed that no detectable dye transfer occurred between the two independent biopsy channels under the tested conditions, demonstrating effective mechanical and fluidic isolation. While the in-vitro experiments validated the feasibility of the proposed DBCR, the experimental setup inevitably simplified certain physiological factors, such as peristalsis, mucosal friction, and luminal fluids. These effects may influence capsule motion in vivo; however, their impact is expected to be limited. The self-locking anchoring mechanism provided sufficient holding force (~0.21 N) to resist typical peristaltic loads (0.05–0.1 N), and each biopsy actuation lasted less than 1s, thereby minimizing disturbance. In practical applications, these limitations primarily affect the quantitative assessment of operational robustness rather than the fundamental feasibility of the proposed design. Future work will focus on in-vivo validation and histological assessment to further evaluate long-term biological safety and clinical performance. Overall, this study presents a comprehensive in-vitro validation of the DBCR, representing an essential step toward future in-vivo application. The proposed design already satisfies the miniaturization and actuation requirements for integration with imaging and localization systems.

Appendix

A video abstract that highlights the key aspects of the work is included. The video demonstrates how the capsule is positioned near the first lesion with the anchor extending out, adjusting its position, and taking a sample at the first lesion. The capsule is guided to the second lesion, and it turns the second needle to the corresponding lesion site. The second needle is extended using control to obtain tissue from the second lesion site.

Acknowledgment

The authors would like to thank Jinping Hu and Shicong Zhang for their input during the experimental setup.

References

[1] M. Rehan, I. Al-Bahadly, D. G. Thomas, W. Young, L. K. Cheng, and E. Avci, "Smart capsules for sensing and sampling the gut: Status, challenges and prospects," *Gut*, vol. 73, no. 1, pp. 186–202, Jan. 2024.

[2] A. F. Peery et al., "Burden and cost of gastrointestinal, liver, and pancreatic diseases in the United States: Update 2021," *Gastroenterology*, vol. 162, no. 2, pp. 621–644, Feb. 2022.

[3] M. Flamant et al., "The prevalence and outcome of jejunal lesions visualized by small bowel capsule endoscopy in Crohn's disease," *Inflammatory Bowel Diseases*, vol. 19, no. 7, pp. 1390–1396, Jun. 2013.

[4] O. M. Ahmed, H. I. Fahim, E. E. Mohamed, and A. Abdel-Moneim, "Protective effects of persea Americana fruit and seed extracts against chemically induced liver cancer in rats by enhancing their antioxidant, anti-inflammatory, and apoptotic activities," *Environ. Sci. Pollut. Res.*, vol. 29, no. 29, pp. 43858–43873, 2022.

[5] A. Koulaouzidis, "Wireless endoscopy in 2020: Will it still be a capsule?," *World J. Gastroenterology*, vol. 21, no. 17, p. 5119, 2015.

[6] P. Valdastri, M. Simi, and R. J. Webster, "Advanced technologies for gastrointestinal endoscopy," *Annu. Rev. Biomed. Eng.*, vol. 14, pp. 397–429, Aug. 2012.

[7] I. M. Mehedi, K. P. Rao, F. M. Alotaibi, and H. M. Alkanfery, "Intelligent wireless capsule endoscopy for the diagnosis of gastrointestinal diseases," *Diagnostics*, vol. 13, no. 8, p. 1445, Apr. 2023.

[8] A. Fritscher-Ravens and C. P. Swain, "The wireless capsule: New light in the darkness," *Digestive Diseases*, vol. 20, no. 2, pp. 127–133, 2002.

[9] Q. Zhang, J. M. Prendergast, G. A. Formosa, M. J. Fulton, and M. E. Rentschler, "Enabling autonomous colonoscopy intervention using a robotic endoscope platform," *IEEE Trans. Biomed. Eng.*, vol. 68, no. 6, pp. 1957–1968, Jun. 2021.

[10] L. Song et al., "Motion control of capsule robot based on adaptive magnetic levitation using electromagnetic coil," *IEEE Trans. Autom. Sci. Eng.*, vol. 20, no. 4, pp. 2720–2731, Oct. 2023, doi: 10.1109/TASE.2022.3201966.

[11] P. Chen, X. He, J. Zhu, and S. Li, "Data-driven control for magnetic actuation capsule: Dynamic compensation and input constraints," *IEEE Trans. Autom. Sci. Eng.*, vol. 22, pp. 4121–4133, 2025, doi: 10.1109/TASE.2024.3407825.

[12] V. H. Le et al., "A novel biopsy capsule endoscope for wireless intestinal tissue collection," in *Proc. Int. Conf. Manipulation, Autom. Robot. at Small Scales (MARSS)*, Jul. 2018, pp. 1–6.

[13] J. Guo, X. Liu, S. Guo, and Q. Fu, "Design and evaluation of a novel magnetoactive biopsy capsule endoscope robot," in *Proc. IEEE Int. Conf. Mechatronics Autom. (ICMA)*, Aug. 2021, pp. 944–949.

[14] M. R. Zarifi Khameneh, Z. Tolouei, M. Yousefi, H. N. Pishkenari, and A. Alasty, "Development and experimental evaluation of an endoscopic capsule robot equipped with a fail-safe biopsy mechanism," in *Proc. 12th RSI Int. Conf. Robot. Mechatronics (ICRoM)*, Dec. 2024, pp. 34–39.

[15] D. Son, H. Gilbert, and M. Sitti, "Magnetically actuated soft capsule endoscope for fine-needle biopsy," *Soft Robot.*, vol. 7, no. 1, pp. 10–21, Feb. 2020.

[16] H. Ito et al., "Fine-needle aspiration biopsy and endoscopic ultrasound for pretreatment pathological diagnosis of gastric gastrointestinal stromal tumors," *Gastroenterology Res. Pract.*, vol. 2012, pp. 1–6, Jan. 2012.

[17] M. Oliveira, H. Araujo, I. N. Figueiredo, L. Pinto, E. Curto, and L. Perdigoto, "Registration of consecutive frames from wireless capsule endoscopy for 3D motion estimation," *IEEE Access*, vol. 9, pp. 119533–119545, 2021.

[18] B. Ye, Z. Zhong, W. Zhang, and D. Hu, "Research on coaxial control of magnetic spiral-type capsule endoscope," *IEEE Access*, vol. 8, pp. 108113–108120, 2020.

[19] M. C. Hoang et al., "DEMA: Robotic dual-electromagnet actuation system integrated with localization for a magnetic capsule endoscope," *Sens. Actuators A, Phys.*, vol. 361, Oct. 2023, Art. no. 114596.

[20] C. D. Natali, T. Ranzani, M. Simi, A. Menciassi, and P. Valdastri, "Trans-abdominal active magnetic linkage for robotic surgery: Concept definition and model assessment," in *Proc. IEEE Int. Conf. Robot. Autom.*, May 2012, pp. 695–700.

[21] V. I. Egorov, I. V. Schastlivtsev, E. V. Prut, A. O. Baranov, and R. A. Turusov, "Mechanical properties of the human gastrointestinal tract," *J. Biomechanics*, vol. 35, no. 10, pp. 1417–1425, Oct. 2002.

[22] Z. Song, W. Zhang, W. Zhang, and D. Paolo, "A novel biopsy capsule robot based on high-speed cutting tissue," *Cyborg Bionic Syst.*, vol. 2022, pp. 1–11, Jan. 2022.

[23] S. Moon, "A planar-type micro-biopsy tool for a capsule-type endoscope using a one-step nickel electroplating process," *Micromachines*, vol. 14, no. 10, p. 1900, Oct. 2023.

[24] E. Karatay, M. Javadov, and H. Kaya, "Thyroid nodule core needle biopsy—Current approach," *Endokrynologia Polska*, vol. 74, no. 6, pp. 591–600, Nov. 2023.

[25] D. Son, M. D. Dogan, and M. Sitti, "Magnetically actuated soft capsule endoscope for fine-needle aspiration biopsy," in *Proc. IEEE Int. Conf. Robot. Autom. (ICRA)*, May 2017, pp. 1132–1139.

[26] S. A. Zargar, M. S. Khuroo, R. Mahajan, G. M. Jan, K. Dewani, and V. Koul, "Endoscopic fine needle aspiration cytology in the diagnosis of gastro-oesophageal and colorectal malignancies," *Gut*, vol. 32, no. 7, pp. 745–748, Jul. 1991.

[27] M. S. Kate, M. M. Kamal, S. K. Bobhate, and A. V. Kher, "Evaluation of fine needle capillary sampling in superficial and deep-seated lesions," *Acta Cytologica*, vol. 42, no. 3, pp. 679–684, 1998.

[28] Z. Liao et al., "Capsule endoscopy practice during the COVID-19 pandemic: Recommendations from the capsule endoscopy group of the Chinese society of digestive endoscopy," *Endoscopy Int. Open*, vol. 9, no. 3, pp. E280–E283, Mar. 2021.

[29] F. Munoz, G. Alici, H. Zhou, W. Li, and M. Sitti, "Analysis of magnetic interaction in remotely controlled magnetic devices and its application to a capsule robot for drug delivery," *IEEE/ASME Trans. Mechatronics*, vol. 23, no. 1, pp. 298–310, Feb. 2018.

[30] M. Hoang et al., "A robotic biopsy endoscope with magnetic 5-DOF locomotion and a retractable biopsy punch," *Micromachines*, vol. 11, no. 1, p. 98, Jan. 2020.

[31] L. J. Sliker, G. Ciuti, M. E. Rentschler, and A. Menciassi, "Frictional resistance model for tissue-capsule endoscope sliding contact in the gastrointestinal tract," *Tribology Int.*, vol. 102, pp. 472–484, Oct. 2016.

[32] B. Ye et al., "A novel magnetic spiral capsule endoscope localization method based on an improved artificial bee colony algorithm," *IEEE Sensors J.*, vol. 24, no. 2, pp. 1740–1750, Jan. 2024.

[33] H. Mateen, R. Basar, A. U. Ahmed, and M. Y. Ahmad, "Localization of wireless capsule endoscope: A systematic review," *IEEE Sensors J.*, vol. 17, no. 5, pp. 1197–1206, Mar. 2017.

[34] H. Zhou and G. Alici, "A novel magnetic anchoring system for wireless capsule endoscopes operating within the gastrointestinal tract," *IEEE/ASME Trans. Mechatronics*, vol. 24, no. 3, pp. 1106–1116, Jun. 2019.

[35] S. Yim, K. Goyal, and M. Sitti, "Magnetically actuated soft capsule with the multimodal drug release function," *IEEE/ASME Trans. Mechatronics*, vol. 18, no. 4, pp. 1413–1418, Aug. 2013.

[36] S. Yim, E. Gultepe, D. H. Gracias, and M. Sitti, "Biopsy using a magnetic capsule endoscope carrying, releasing, and retrieving untethered microgrippers," *IEEE Trans. Biomed. Eng.*, vol. 61, no. 2, pp. 513–521, Feb. 2014.

[37] V. H. Le et al., "Electromagnetic field intensity triggered micro-biopsy device for active locomotive capsule endoscope," *Mechatronics*, vol. 36, pp. 112–118, Jun. 2016.

[38] K. Kong, S. Yim, S. Choi, and D. Jeon, "A robotic biopsy device for capsule endoscopy," *J. Med. Devices*, vol. 6, no. 3, Sep. 2012, Art. no. 031004.

[39] M. Simi, G. Gerboni, A. Menciassi, and P. Valdastri, "Magnetic torsion spring mechanism for a wireless biopsy capsule," *J. Med. Devices*, vol. 7, no. 4, Dec. 2013, Art. no. 041009.

[40] D. Ye et al., "Design and control of a magnetically-actuated capsule robot with biopsy function," *IEEE Trans. Biomed. Eng.*, vol. 69, no. 9, pp. 2905–2915, Sep. 2022.

[41] H. Leon-Rodriguez, S.-H. Park, and J.-O. Park, "Testing and evaluation of foldable biopsy tools for active capsule endoscope," in *Proc. 20th Int. Conf. Control, Autom. Syst. (ICCAS)*, Oct. 2020, pp. 473–479.

[42] L. J. Haseler, R. R. Sibbitt, W. L. Sibbitt, A. A. Michael, C. M. Gasparovic, and A. D. Bankhurst, "Syringe and needle size, syringe type, vacuum generation, and needle control in aspiration procedures," *CardioVascular Interventional Radiol.*, vol. 34, no. 3, pp. 590–600, Jun. 2011.

[43] V. Narang, A. Jindal, A. Singh, B. Varun Mehta, N. Sood, and A. Sood, "Diagnostic utility of multiple site duodenal biopsies in celiac disease," *Indian J. Pathol. Microbiology*, vol. 64, no. 5, p. 73, 2021.

[44] H.-J. Yang et al., "Sample collection methods in upper gastrointestinal research," *J. Korean Med. Sci.*, vol. 38, no. 32, p.255, and 1–14, 2023.

[45] I. de Sio et al., "Ultrasound-guided percutaneous biopsy for diagnosis of gastrointestinal lesions," *Digestive Liver Disease*, vol. 45, no. 10, pp. 816–819, Oct. 2013.

[46] M. Nakao, M. Nakamura, T. Mizowaki, and T. Matsuda, "Statistical deformation reconstruction using multi-organ shape features for pancreatic cancer localization," *Med. Image Anal.*, vol. 67, Apr. 2021, Art. no. 101829, doi: 10.1016/j.media.2020.101829.

[47] J. M. Hostetter and F. A. Uzal, "Gastrointestinal biopsy in the horse: Overview of collection, interpretation, and applications," *J. Veterinary Diagnostic Invest.*, vol. 34, no. 3, pp. 376–388, May 2022.

[48] Q. Cao et al., "A dual-functional capsule robot for drug delivery and tissue biopsy based on magnetic torsion spring technology," *Bio-Des. Manuf.*, vol. 8, no. 3, pp. 495–510, 2025, doi: 10.1631/bdm.\break2400276.

[49] F. Niu, Z. Li, H. Wang, Y. Qian, Y. Li, and P. Song, "Hierarchical control for real-time 3D manipulation of magnetic bead using a single permanent magnet," *IEEE Robot. Autom. Lett.*, vol. 11, no. 1, pp. 834–841, Jan. 2026, doi: 10.1109/LRA.2025.3629982.